INHIBITION OF CORROSION ON AA2024-T3 BY RARE EARTHS & MERCAPTOACETATE

R. Catubig[1], M. Forsyth[1], B. Hinton[1], I. Cole[2], A. Hughes[2]
[1]Deakin University, [2]CSIRO, Melbourne, Australia

SUMMARY: The use of the aluminium alloy AA2024-T3 has long been associated with a strong vulnerability to localised corrosion. Dealloying and pitting corrosion can occur on and around intermetallic particles when exposed to aggressive environments such as sodium chloride electrolytes. Specific combinations of rare earths and organic compounds have demonstrated strong synergistic inhibition on the AA2024-T3 alloy. This work has focused on rare earths and organic compounds containing thiol functional groups. It is believed that the sulphur in the thiol group can form protective films over the surface of copper-rich intermetallic particles due to the affinity between copper and sulphur. Previous studies with the multiwell tests have identified that solutions containing sodium mercaptoacetate provided strong inhibition at pH 3 and 6. This work presents the initial findings from the polarisation tests and constant immersion corrosion experiments in the presence of sodium mercaptoacetate.

Keywords: AA2024-T3, cerium, praseodymium, mercaptoacetate

1. INTRODUCTION

The use of the AA2024-T3 alloy within the aerospace industry is well documented, predominantly due to its high strength-to-weight ratio and fracture toughness [1-3]. Intermetallic (IM) particles embedded within the aluminium matrix are responsible for the relatively high strength. The heterogeneous nature of the alloy surface, due to the presence of these IM particles, enables numerous microgalvanic cells to be established which can lead to localised corrosion such as dealloying and pitting. Localised corrosion can lead to more severe modes of corrosion. Intergranular attack and microcrack formation are examples of phenomena that can severely limit the mechanical integrity of the alloy over time.

A cost effective method of protecting these alloys from localised corrosion is with the use of inhibitors. One of the most effective is chromate ions [4], however, their high toxicity and carcinogenic properties have led to strict regulations on their use [5]. A number of potential alternatives have been studied to date [6-11] but the inhibitor combination of a rare-earth (RE) metal with an appropriate organic compound has shown very strong synergistic inhibition on mild steel and the AA2024 aluminium alloy [12-17]

Copper (Cu) is a major alloying element in AA2024-T3 and a number of Cu-containing IM particles have been found to have a strong influence on the localised corrosion of this alloy [3, 18, 19]. It is hypothesised that a combination of a RE with a thiol-containing organic compound will provide effective corrosion protection by targeting these Cu-rich IM particles. The strong affinity between sulphur and Cu [20] means that these inhibitors will react preferentially with Cu-rich IM particles providing protection at these sites. In this work, a number of thiol-containing (-SH) compounds [9] were selected to be coupled with the RE chlorides, cerium (Ce) and praseodymium (Pr) due to their inhibiting effects as shown in the literature [11, 21]. This work will shed light on whether protection of these IM particles will lead to more effective inhibition on the AA2024-T3 alloy.

2. EXPERIMENTAL DETAILS

2.1. Materials

The same batch of commercially available AA2024-T3 alloy sheet with a thickness of 2.7 mm was used in all experiments. Inductively Coupled Plasma Optical Emission Spectroscopy results identified 4.63 wt% of Cu and 1.39 wt% of magnesium present in the alloy. All inhibitors were dissolved with 0.1 M sodium chloride (NaCl) in deionised water. Sodium mercaptoacetate (Na-MAcet) was mixed with $CeCl_3 \cdot 7H_2O$ or $PrCl_3 \cdot 6H_2O$ to identify which combination demonstrated the most effective inhibition.

2.1. Multiwell Corrosion Test

This method was developed by White et al. [22]. A plate of AA2024-T3 was abraded with Scotch-Brite under tap water and dried with lint-free tissues. A polydimethylsiloxane block with holes (which acted as wells) was clamped over the AA2024-T3 plate. Different volumes of the RE chlorides and Na-MAcet were mixed in each well in a microplate to dilute each solution to the desired concentrations. The pH of the solutions were adjusted with hydrochloric acid or sodium hydroxide prior to mixing in the microplate. The mixed solutions were transferred into the corresponding well over the alloy plate and left to sit for 24 hours. Upon the completion of the experiment, the plate was rinsed with deionised water, dried with compressed air and optical images were taken. The images were edited in Adobe Photoshop in order to combine the visual effects of pitting and the formation of corrosion product in one image. Pitting tended to darken the AA2024-T3 alloy surface while the formation of hydroxides and oxides of aluminium would give a whitening effect. Both the pitting and the formation of corrosion product were used as indicators for corrosion. Corrosion rankings for each well were obtained by comparing the polished alloy surface with the corroded well surface. The details of the procedure were reported by White et al. [22]. The corrosion rankings ranged between 0-10 whereby 0 is no corrosion and 10 representing the highest level of corrosion observed amongst the wells. i.e. a ranking of 10 would correspond to the darkest well in the analysis compared to the bare alloy.

2.2. Potentiodynamic Polarisation

A 10 mm x 10 mm surface area of the AA2024-T3 alloy was mounted into epoxy and polished to 1 μm with alumina powder. A standard three electrode cell was used with titanium mesh as the counter electrode (700 mm^2) and saturated calomel electrode as the reference electrode. Each sample was immersed in 400 ml test solution for 30 mins before starting the polarisation scan. The potential range was -0.3 to 0.5 V relative to the open circuit potential at a scan rate of 0.1667 mV/s. Each test was performed in triplicate. The solutions tested are shown in Table 1.

Table 1. Composition of the test solutions for both the polarisation experiments and the immersion tests

Solution Components	Concentration (M)			
	[NaCl]	[$CeCl_3$]	[$PrCl_3$]	[Na-MAcet]
NaCl (Control)	0.1	-	-	-
Sodium mercaptoacetate (3Na-MAcet)	0.1	-	-	$3x10^{-4}$
$CeCl_3$	0.1	$1x10^{-4}$	-	-
$PrCl_3$	0.1	-	$1x10^{-4}$	-
$CeCl_3$ + Na-MAcet (Ce+3MAcet)	0.1	$1x10^{-4}$	-	$3x10^{-4}$
$PrCl_3$ + Na-MAcet (Pr+3MAcet)	0.1	-	$1x10^{-4}$	$3x10^{-4}$

2.3. Optical Microscopy after 7 days of Immersion

Epoxy mounted AA2024-T3 samples with an area of 10 mm x 10 mm were polished to 1 μm alumina powder. 40 ml of the solutions listed in Table 1, were made up and placed in separate beakers. A polished sample was fully immersed into each solution and left to sit open to air for 7 days. These samples were rinsed with deionised water and dried with nitrogen gas upon completion of the testing period. Optical microscopy images were taken of each sample.

3. RESULTS

3.1 Multiwell Test Inhibitor Screening

A number of thiol-containing organic compounds were selected from the study of Harvey et al. [9] due to their inhibiting performance with the AA2024-T3 alloy. In the current work, the solutions containing only Na-MAcet appeared to consistently provide strong inhibition at pH 3 and when RE chlorides was added, improved inhibition was observed at pH 6. Different ratios of RE chlorides to Na-MAcet were tested and the most effective was found to be 1:3 (to be published).

Figure 1 show the corrosion rankings obtained from the multiwell experiments for the solutions containing no inhibitor (0.1M NaCl control), $CeCl_3$, $PrCl_3$, 3Na-MAcet on its own, and the mixtures of Ce+3MAcet and Pr+3MAcet. In general, the level of corrosion increased with increasing pH and the mixture Pr+3MAcet provided greater inhibition than the solutions containing Ce+3MAcet at all the tested pH conditions. The increase of corrosion was more gradual for the mixtures. $CeCl_3$ was the exception as the best performance was observed at pH 6 but worst at pH 8.5 for $CeCl_3$.

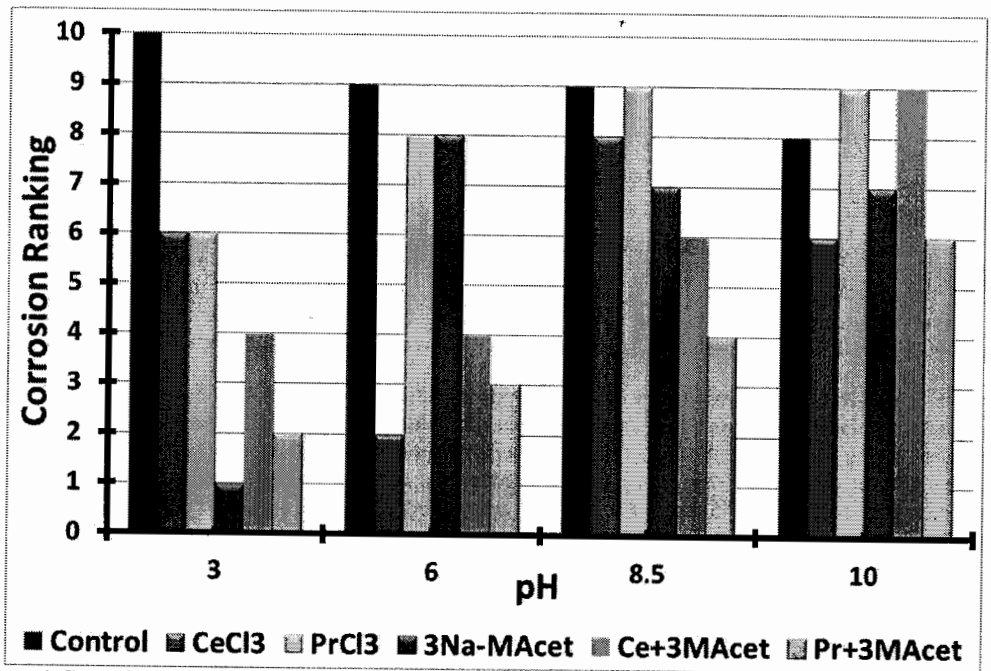

Figure 1 Corrosion rankings from the multiwell corrosion tests for the solutions of 3Na-MAcet (red), $CeCl_3$ (purple), $PrCl_3$ (green), Ce+3MAcet (orange) and Pr+3MAcet (blue)

3.2 Potentiodynamic Polarisation at pH 6

Figure 2 shows the typical polarisation graphs at pH 6 for solutions containing no inhibitor (control), $CeCl_3$ at $1x10^{-4}$M, Na-MAcet at $3x10^{-4}$M and the mixture of $CeCl_3$ and Na-MAcet (Ce+3MAcet) at $1x10^{-4}$M and $3x10^{-4}$M respectively. Only measurements at pH 6 were presented here since some inhibitors (such as $CeCl_3$) showed strong inhibition under this pH condition. Testing at acidic and alkaline environments is still underway. Testing at pH 6 was intended to simulate the near neutral condition to be compared to the performances in the acidic (pH 3) and alkaline (pH 10) environment. Nevertheless near-neutral pH is still of significance since this will be the initial pH in many situations. In the presence of 3Na-MAcet, the polarisation curve was cathodically shifted to more negative potentials with respect to the control. Since the current density of the anodic arm was at more positive current densities and the cathodic arm currents can be seen as identical to the control, 3Na-MAcet appeared to accelerate anodic kinetics on the AA2024-T3 alloy under the test conditions. $CeCl_3$ decreased the current density of the cathodic arm by more than an order of magnitude, while no significant effect was observed on the anodic arm. $CeCl_3$ also shifted the curve to more negative potentials possibly due to its dominating effect on the cathodic reaction.

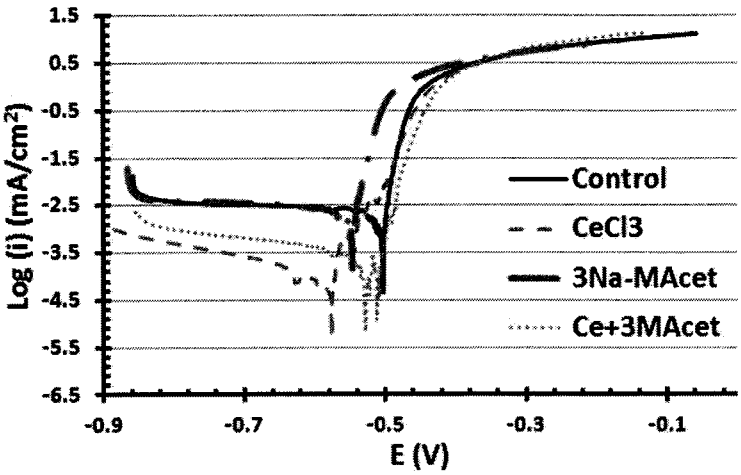

Figure 2 Polarisation graphs, Control (black), $CeCl_3$ (purple dashed line), 3Na-MAcet (red dashed line) and Ce+3MAcet (orange dotted line) at pH 6

The mixture containing Ce+3MAcet significantly reduced the cathodic reaction as can be seen by the reduction in current density of the cathodic arm. It must be noted that the mixture reduced the current density of the cathodic arm to a lesser extent than the $CeCl_3$ but it had a stronger effect on the anodic arm between the potentials -0.5 and -0.4 V, where there is a clear difference between $CeCl_3$ and the mixture Ce+3MAcet.

The control and Na-MAcet curves shown in Figure 2 are also displayed in Figure 3 alongside the scans for the inhibitors $PrCl_3$ and Pr+3MAcet. Both the solutions containing $PrCl_3$ ($PrCl_3$ $1x10^{-4}$ M and Pr+3MAcet) demonstrated strong cathodic inhibition by the decreased current density on the cathodic arm. Similar to the case of the Ce+3MAcet mixture, Pr+3MAcet could not reduce the cathodic current more negative than $PrCl_3$. In addition, between potentials -0.5 and -0.4 V, there was a reduction in current density for the Pr+3MAcet compared to $PrCl_3$.

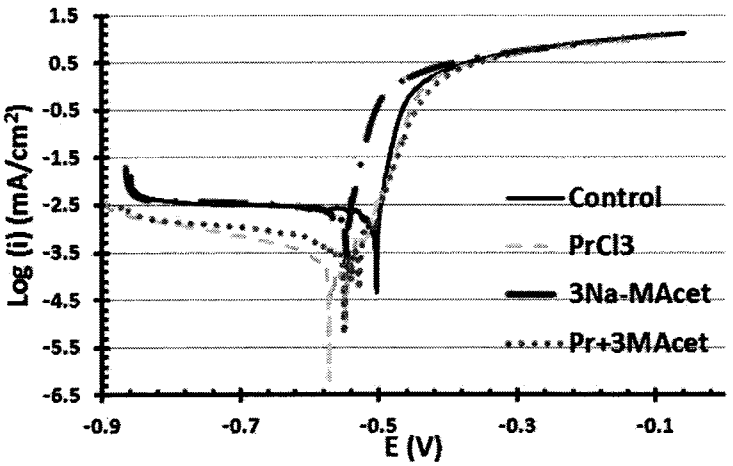

Figure 3 Polarisation curves for the solutions containing the Control (black), $PrCl_3$ (green dash line), 3Na-MAcet (red dashed line) and Pr+3MAcet (blue dotted line) at pH 6

The average i_{corr} values for each of the inhibitors are shown in Figure 4. The average i_{corr} value of 3Na-MAcet was higher than the control which supports the possibility that corrosion was accelerated in the presence of 3Na-MAcet. $CeCl_3$ produced the lowest i_{corr} and thus the lowest corrosion rate. The mixtures containing both a RE chloride and 3Na-MAcet yielded significant reductions in i_{corr} compared to the control and the solution containing 3Na-MAcet on its own in solution. $PrCl_3$ showed similar reductions in i_{corr} to $CeCl_3$. On the other

hand, under these conditions the mixtures were not able to produce average i_{corr} values lower than the RE chloride salts indicating that over the whole surface, corrosion inhibition was not as effective with the mixtures.

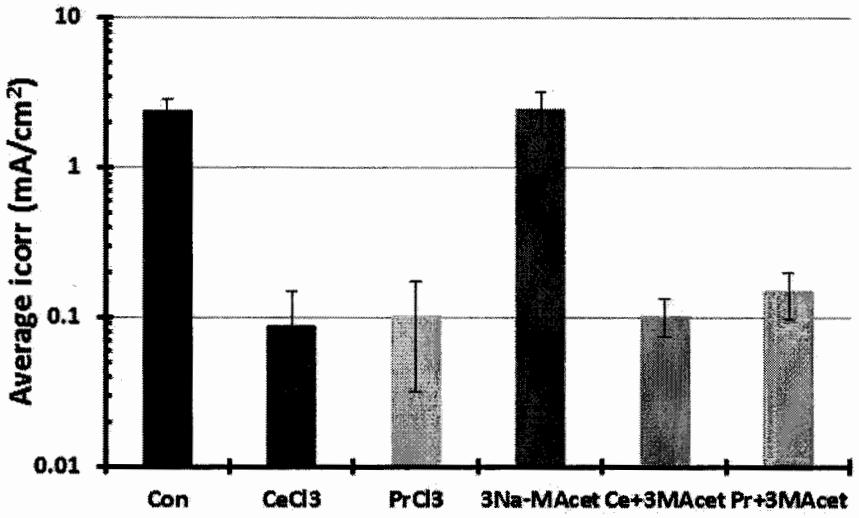

Figure 4 Average i_{corr} values for each solution, 0.1M NaCl control (black), $CeCl_3$ (purple), $PrCl_3$ (green), 3Na-MAcet (red), Ce+3MAcet (orange) and Pr+3MAcet (blue).

This is in contrast to the well experiments where distinct differences were observed. For example, Ce+3MAcet gave a higher level of corrosion than Pr+3MAcet on the multiwell tests but the reverse was observed in terms of the average i_{corr} value. This difference in the polarisation and the multiwell data could be due to the duration of each test since the multiwell test was a 24 hour test while the polarisation test was a maximum of 3 hours. Further tests must be done to observe the effects of immersion time.

3.3 Optical Microscopy after 7 days of Immersion

Images of the immersion samples were taken using an optical microscope and shown in Figure 5. Large amounts of corrosion product had deposited onto the surface of the control sample. This made it difficult to see the surface of the alloy and removal of this layer will be done after all testing of this surface layer has been completed. The sample immersed in $3x10^{-4}$M Na-MAcet for 7 days featured pits of varied diameters throughout the whole of the AA2024-T3 surface (examples are shown by the green arrows). The polarisation experiments showed that the Na-MAcet inhibitor had an average i_{corr} value that was approximately equal to the control samples. Due to the lack of visibility on the control sample, confirmation of a correlation between the immersion samples and the polarisation results cannot be made at this time.

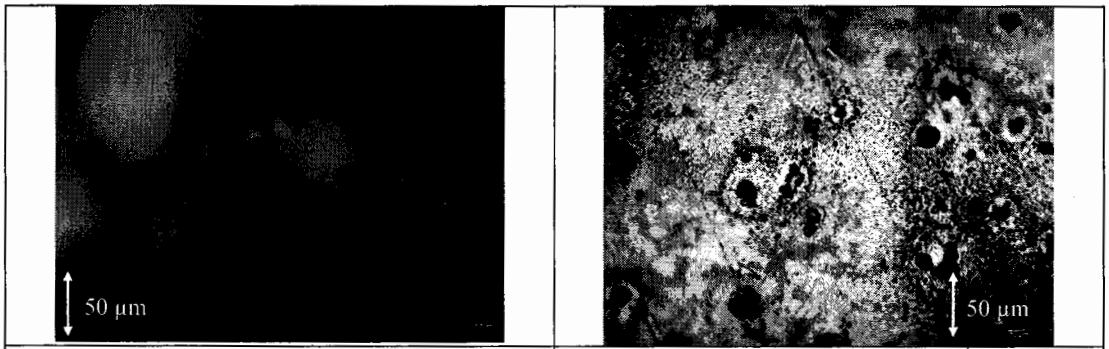

Control 0.1M NaCl	0.1 M NaCl + Na-MAcet $3x10^{-4}$ M

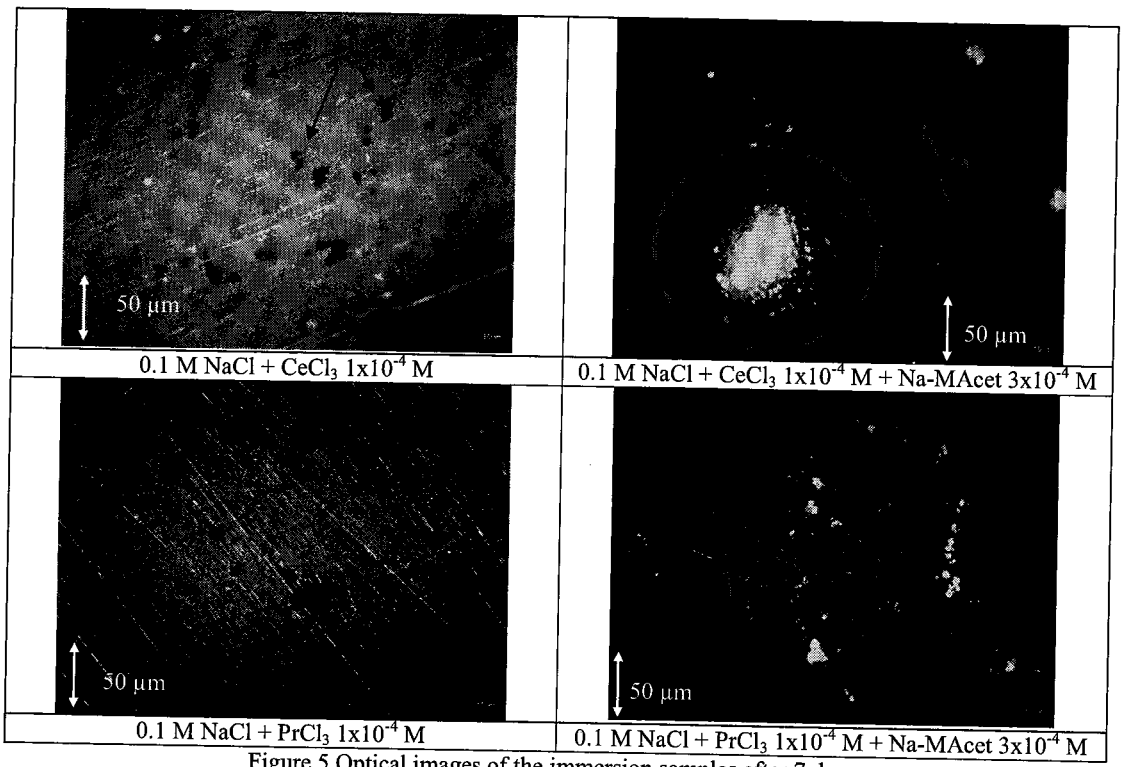

Figure 5 Optical images of the immersion samples after 7 days.

Several dark spots were found on the samples immersed in the RE chloride solutions ($CeCl_3$ and $PrCl_3$) and the scratch marks from the polishing process can still be identified. The red arrows shown in Figure 5 give examples of these dark spots observed. Corrosion product was almost non-existent on the surface except at a number of specific sites.

Similar to the RE chlorides, corrosion product seemed to only deposit at certain sites with the mixed solutions (Ce+3MAcet and Pr+3MAcet). The level of corrosion product over these sites seemed to be noticeably greater compared to the RE chlorides. This is particularly obvious with the Ce+3MAcet sample where a large amount of corrosion product was found over the site circled in red. Small deposits were also found over the surrounding matrix. The Pr+3MAcet also showed a greater amount of corrosion product compared to the RE chlorides but not to the extent of the Ce+3MAcet mixture The relatively strong level of inhibition can be seen by the significant reductions in pitting and corrosion damage in the presence of the RE chloride solutions.

4. DISCUSSION

4.1. Strong Inhibition by Na-MAcet at pH 3

From the multiwell results (Figure 1), the strong inhibition at pH 3 and the increase in corrosion between pH 3 and 6 is not well understood at this stage of the project. Seter et al. [17] have shown that the dominant species in solution of the inhibitor, $La(4OH\text{-}Cin)_3$, changes with pH. In addition, the level of inhibition was also affected by the pH whereby the higher efficiencies of inhibition were observed at more alkaline conditions. Na-MAcet may have certain species with strong corrosion inhibiting properties present at pH 3 but not present at higher pH levels. This could be the reason as to why strong inhibition was only observed at pH 3.

In the literature, mercaptoacetic acid was found to increase corrosion under sufficiently acidic conditions. Abiola et al. proposed that mercaptoacetic acid became protonated when added to 0.5 M hydrochloric acid leading to increased hydrogen evolution reaction rates on the 3SR aluminium alloy [23]. Mahgoub concluded that increased protonation limited the ability of the inhibitor to adsorb onto steel [24]. Abd El-Rahman found that corrosion rates on zinc would rise as the concentration of mercaptoacetic acid increased [25]. This was attributed to faster cathodic kinetics due to the higher concentration of hydrogen ions. In the case of Na-MAcet, it is still unknown as to why corrosion inhibition, not corrosion acceleration, was observed at pH 3. Horner

stated that the structure of an inhibitor as well as the spatial separation between functional groups will have a strong influence on the corrosion efficiency [26]. This was confirmed by Harvey et al. who found small changes in molecular structure, such as the site that functional groups were bonded, led to significant changes in corrosion inhibition [9]. The results in this work could be implying that as the sodium salt, the structure of Na-MAcet allowed for effective corrosion inhibition for the AA2024-T3 alloy at pH 3, while the structure of mercaptocetic acid promoted corrosion.

4.2. Effect of Mixing Na-MAcet with Rare Earth Chlorides at pH 6

It was originally hypothesised that stronger inhibition of localised corrosion on the AA2024-T3 alloy could be achieved by combining a RE metal and a thiol-containing organic compound as an inhibitor. Thiol-containing organic compounds were selected to incorporate sulphur into the inhibitor mixtures. As mentioned in the introduction, the Cu-rich IM particles are known to have a strong influence on the corrosion of the AA2024-T3 alloy. The sulphur would give the inhibitor "smart" capabilities enabling it to preferentially inhibit corrosion of the IM particles.

With the i_{corr} values obtained with the RE salts being lower than those for the mixtures (Figure 4), analysis of the polarisation curves could easily lead to misleading conclusions that more powerful inhibition through mixing a RE chloride and Na-MAcet was not obtained. The mixtures, Ce+3MAcet and Pr+3MAcet, consistently reduced the corrosion current density of the anodic arm to more negative currents compared to $CeCl_3$ and $PrCl_3$ respectively as well as Na-MAcet. The significant difference in current density can be seen between potentials of -0.4 to -0.5 V. This may indicate that the mixture inhibits corrosion in a different manner to that of the RE chlorides or Na-MAcet when tested separately. One can argue that this improvement in anodic inhibition could be due to the RE chlorides and Na-MAcet providing some synergic effect. It is known that the species of an inhibitor present in solution can have a large effect on the level of inhibition, and it is likely that the same applied in the case of RE chlorides mixed with Na-MAcet. The level of cathodic inhibition provided by the mixtures were not as strong compared to the RE chlorides leading to i_{corr} values of the mixtures being more positive in current density. However a stronger level of anodic inhibition for the mixtures is still significant as it may be more effective under different conditions. In a system where the limiting factor was the anodic reactions, the mixtures may prove to be a more effective inhibitor. Another factor to consider was that the concentrations used in this work may not have been the optimum concentration of these inhibitors. This will be a subject of a later study.

In Figure 1, Pr+3MAcet yielded lower corrosion rankings compared to Ce+3MAcet for all pH conditions, indicating that the former was providing greater inhibition. In contrast, Ce+3MAcet reduced the average i_{corr} value to more negative current densities compared to the Pr+3MAcet (Figure 4). It must be remembered that there was a significant difference in the time that the alloy was in contact with the test solutions. Blin et al. found that the mode of inhibition of $La(4OH\text{-}cin)_3$ changed from predominantly anodic to cathodic over time [14]. Forsyth et al. observed a similar behaviour with Ce salicylate [13]. The effectiveness of the inhibitor was also affected by the time that the alloy was immersed with the inhibitor. It is possible that upon early exposure, Ce+3MAcet was providing more effective inhibition as observed in the polarisation data. But over time, Pr+3MAcet was able to protect the AA2024-T3 alloy more effectively giving the lower corrosion rankings in the multiwell test. The time dependency of these inhibitors needs to be confirmed along with many observations discussed in this paper. Further work must be done to better understand how the inhibitor system with Na-MAcet and the RE chlorides provide inhibition when mixed together in solution. These include the possible dependence of inhibition towards time, concentration and structure changes such as protonation.

5. CONCLUSIONS

RE chlorides in solution were found to be more effective in limiting the corrosion current density of AA2024-T3 in 0.1 M NaCl compared to mixtures of RE chlorides and Na-MAcet. A significant level of anodic inhibition was observed with the mixture of inhibitors between -0.4 and -0.5 V and there seemed to be a time dependence of inhibition for the Pr+3MAcet mixture. This work is only in its infancy thus the mechanisms and behaviour of the inhibitors are currently not completely understood. The level of inhibition obtained by the Ce+3MAcet and Pr+3MAcet mixtures, as seen by the immersion tests and the polarisation data, show great potential as an inhibitor but it is obvious that a great deal of work is still required before any solid conclusions can be made.

6. REFERENCES

1. Bauccio M. ASM metals reference book. 3rd ed., ASM International (Publisher) Ohio, 1993.
2. Vargel C. Corrosion Of Aluminium. Elsevier (Publisher), Oxford, 2004.
3. Muster TH, Hughes AE, Thompson GE. Copper distribution in aluminium alloys in corrosion research trends, Nova Science (Publishers) New York, 2007.
4. Baldwin KR, Gibson MC, Lane PL, Smith CJE, editors. The development of Alternatives to Chromate Inhibitors for the Protection of Aerospace Aluminium Alloys. 7th European Symposium on Corrosion Inhibitors (7SEIC); 1990; University of Ferrara, Italy.
5. Twite RL, Bierwagen GP. Review of Alternatives to Chromate for Corrosion Protection of Aluminum Aerospace Alloys. Prog Org Coat. 1998 1998;33(2):91-100.
6. Hughes AE, Cole IS, Muster TH, Varley RJ. Designing green, self-healing coatings for metal protection. NPG Asia Materials. 2010;2(4):142-51.
7. Osborne JH, Blohowiak KY, Taylor SR, Hunter C, Bierwagon G, Carlson B, et al. Testing and evaluation of nonchromated coating systems for aerospace applications. Prog Org Coat. 2001 May;41(4):217-25.
8. Kendig MW, Buchheit RG. Corrosion inhibition of aluminum and aluminum alloys by soluble chromates, chromate coatings, and chromate-free coatings. Corrosion. 2003 May;59(5):379-400.
9. Harvey TG, Hardin SG, Hughes AE, Muster TH, White PA, Markley TA, et al. The effect of inhibitor structure on the corrosion of AA2024 and AA7075. Corrosion Sci. [Article]. 2011 Jun;53(6):2184-90.
10. Hinton BRW, Arnott DR, Ryan NE. The inhibition of aluminium-alloy corrosion by cerous cations. Metals Forum. 1984;7(4):211-7.
11. Hinton BRW. Corrosion inhibition with rare-earth-metal salts. J Alloy Compd. 1992 Mar;180:15-25.
12. Forsyth M, Wilson K, Behrsing T, Forsyth C, Deacon GB, Phanasgoankar A. Effectiveness of rare-earth metal compounds as corrosion inhibitors for steel. Corrosion. 2002 Nov;58(11):953-60.
13. Forsyth M, Forsyth CM, Wilson K, Behrsing T, Deacon GB. ATR characterisation of synergistic corrosion inhibition of mild steel surfaces by cerium salicylate. Corrosion Sci. 2002;44(11):2651-6.
14. Blin F, Leary SG, Wilson K, Deacon GB, Junk PC, Forsyth M. Corrosion mitigation of mild steel by new rare earth cinnamate compounds. J Appl Electrochem. [Article]. 2004 Jun;34(6):591-9.
15. Ho D, Brack N, Scully J, Markley T, Forsyth M, Hinton B. Cerium dibutylphosphate as a corrosion inhibitor for AA2024-T3 aluminum alloys. J Electrochem Soc. [Article]. 2006;153(9):B392-B401.
16. Markley TA, Forsyth M, Hughes AE. Corrosion protection of AA2024-T3 using rare earth diphenyl phosphates. Electrochim Acta. 2007;52(12):4024-31.
17. Seter M, Hinton B, Forsyth M. Understanding speciation of lanthanum 4-hydroxy cinnamate and its impact on the corrosion mechanism for AS1020 steel. 2012 January;159(4):C1-C9.
18. Boag A, Hughes AE, Glenn AM, Muster TH, McCulloch D. Corrosion of AA2024-T3 Part I. Localised corrosion of isolated IM particles. Corrosion Sci. 2011;53(1):17-26.
19. Rao KS, Rao KP. Corrosion resistance of AA2219 aluminium alloy: electrochemical polarisation and impedance study. Materials Science and Technology. 2006;22(1):97-104.
20. Sastri VS. Green Corrosion Inhibitors: Theory and Practice: John Wiley & Sons; 2011.
21. Markley TA, Hughes AE, Ang TC, Deacon GB, Junk P, Forsyth M. Influence of praseodymium - Synergistic corrosion inhibition in mixed rare-earth diphenyl phosphate systems. Electrochem Solid State Lett. [Article]. 2007;10(12):C72-C5.
22. White PA, Smith GB, Harvey TG, Corrigan PA, Glenn MA, Lau D, et al. A new high-throughput method for corrosion testing. Corrosion Sci. 2012;58:327-31.
23. Abiola OK, Oforka NC, Angaye SS. Corrosion behaviour of aluminium in hydrochloric acid (HCl) solution containing mercaptoacetic acid. Materials Letters. [Article]. 2004 Nov;58(27-28):3461-6.
24. Mahgoub FM. Effect of protonation on the inhibition efficiency of thiourea and its derivatives as corrosion inhibitors. Anti-Corros Methods Mater. 2008 2008;55(6):324-8.
25. Abd El-Rahman HA, Gad-Allah AG, Tamous H. Corrosion of zinc in acetic acid derivatives: Glycolic, mercaptoacetic and cyanoacetic acids and glycine. Materialwiss. Werkstofftech. 1998;29(5):263-9.
26. Horner L, Meisel K. Corrosion Inhibitors 23(1) - Does There Exist a Structure-Efficiency Relation in the Organic Inhibitors of Aluminium Corrosion? Wekst Korros. 1978 1978;29(10):654-64.

7. AUTHOR DETAILS

R. Catubig graduated as a Materials Engineer from Monash University in Victoria, Australia. He is currently undertaking his PhD studies under the supervision of Maria Forsyth, Bruce Hinton, Tony Hughes and Ivan Cole. For his Honours project, he studied the effects of lanthanum hydroxy cinnamate on filiform corrosion. His PhD project attempts to understand the mechanisms of inhibition by novel rare earth inhibitors on the aerospace alloy, AA2024-T3.

Professor M. Forsyth is the Associate Director of ARC Centre of Excellence for Electromaterials Science. Her research is directed towards development and understanding of charge transport at metal/electrolyte interfaces and within electrolyte materials. These include a wide range of ionic liquids, polymer electrolytes and plastic crystals. Using this understanding, her team collaborates very productively with colleagues within academia, CSIRO, DSTO as well as industry to design new materials and processes to control and optimise these phenomena in two key areas - corrosion and electrochemical devices.

Professor B. Hinton is a well-known figure in metal finishing, corrosion processes, inhibition and prevention. Though Bruce is currently retired, during his career as Principal Research Defence scientist he provided great contributions to several organisations in prevention of corrosion, specifically on aircraft structures. He continues to give advice and support to research and students alike to this day.

Dr I. Cole is a Chief Research Scientist at CSIRO and was previously the Deputy Chief of the CMSE division. His depth of expertise in material science and mathematical modelling allowed him to work in areas such as manufacturing and aerospace alloy corrosion protection. He was awarded the Silver Medal, BAE Systems Chairman's Award for Innovation and the Guy Benough Award throughout the course of his career. He remains at CSIRO, offering his skill and knowledge to colleagues and students.

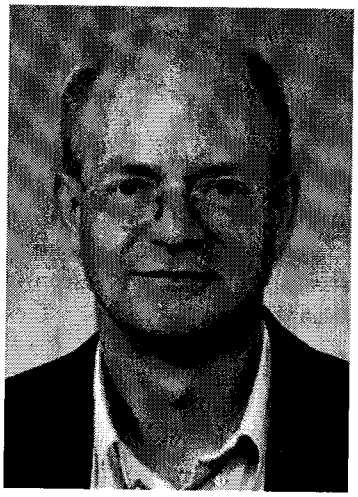

Dr A. Hughes has been involved in multiple studies during the course of his career, such as surface science, metal finishing, alloy corrosion and corrosion inhibition. He has been awarded with the BAE SYSTEMS Chairman's Silver Award for Innovation as well as an award for Innovation from CSIRO. He remains at CSIRO lending his expertise not only to industrial partners but also to students and interns.